ACS Biomaterials SCIENCE & ENGINEERING

Article

Cite This: ACS Biomater. Sci. Eng. 2018, 4, 1463−1470

Silk-Based Aqueous Microcontact Printing

Baskaran Ganesh Kumar,[†] Rustamzhon Melikov,[†] Mohammad Mohammadi Aria,[‡] Aybike Ural Yalcin,[§] Efe Begar,[∥] Sadra Sadeghi,[⊥] Kaan Guven,[§] and Sedat Nizamoglu*[,†,‡,⊥]

[†]Department of Electrical and Electronics Engineering, Koc University, Istanbul 34450, Turkey

[‡]Graduate School of Biomedical Engineering, Koc University, Istanbul 34450, Turkey

[§]Department of Physics, Koc University, Istanbul 34450, Turkey

[∥]Department of Molecular Biology and Genetics, Koc University, Istanbul 34450, Turkey

[⊥]Graduate School of Material Science and Engineering, Koc University, Istanbul 34450, Turkey

Supporting Information

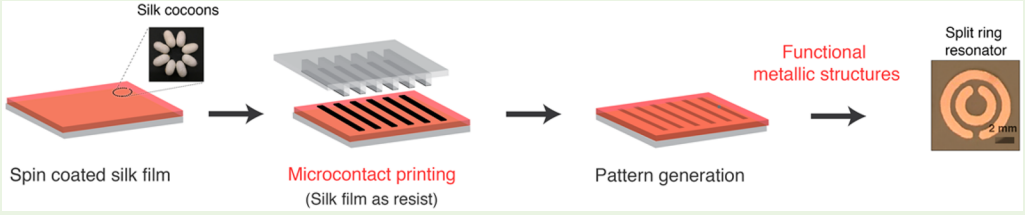

ABSTRACT: Lithography, the transfer of patterns to a film or substrate, is the basis by which many modern technological devices and components are produced. However, established lithographic approaches generally use complex techniques, expensive equipment, and advanced materials. Here, we introduce a water-based microcontact printing method using silk that is simple, inexpensive, ecofriendly, and recyclable. Whereas the traditional microcontact printing technique facilitates only negative lithography, the synergetic interaction of the silk, water, and common chemicals in our technique enables both positive and negative patterning using a single stamp. Among diverse application possibilities, we exemplify a proof of concept of the method through optimizing its metal lift-off process and demonstrate the fabrication of electromagnetic metamaterial elements on both solid and flexible substrates. The results indicate that the method demonstrated herein is universally applicable to device production and technology development.

KEYWORDS: *microfabrication, microcontact printing, silk lithography, resource limited settings, lithography*

INTRODUCTION

Methods, devices, and components for resource limited/poor settings have significant potential to improve the health, education, economy, and quality of lives in developing countries.[1−3] Resource-limited settings demand a dedicated approach of the current technologies because skilled labors are rare, laboratory infrastructure is inadequate, and maintenance of sophisticated equipment is economically not feasible.[4] For that, recently a wide variety of techniques and devices have been developed for resource-limited settings such as smart phone sensors,[5−7] paper-based microfluidics,[1,8,9] and hand-powered devices (e.g., egg beater) as a centrifuge, which are in general simple, inexpensive, locally available, and easily transportable.[1−3,10−12]

Today, lithography is an essential process to generate components and devices at all scales, and resource-limited settings require lithographic techniques that are characterized by a simple process flow, nontoxic materials, sustainable resources, and low material and fabrication cost. Inspired by microcontact printing[13−15] and the ancient material silk,[16,17] we introduce a lithographic technique for resource-limited settings. Silk has been successfully applied to various lithographic methods,[18−33] including electron beam lithography,[19,25] soft-lithography,[34−36] and photolithography;[37−39] however, these methods require complex and skill-intensive processing steps and expensive instrumentation. Thus, we present here a simple, inexpensive, quick, portable, and convenient method for generating micropatterns on both planar and flexible surfaces. We use common chemicals as inks (e.g., methanol and ethanol), water as the developer, and cloth/filter paper as the ink pad; in addition, silk, which serves as the resist, is easily accessible because of its local and large-scale production by almost the entire world, such as the Silk Road countries, Africa, and South America. It is ecofriendly because of its proteomic origin and recyclable after lithography. Whereas only negative lithography is possible in conventional microcontact printing because of gold-alkanethiol interactions,[40] both positive and negative lithography are achievable using silk microcontact printing by using a single stamp. Furthermore, the silk resist used in this method enables selective lift-off and the generation of functional electromagnetic structures.

Received: January 12, 2018
Accepted: March 7, 2018
Published: March 7, 2018

DOI: 10.1021/acsbiomaterials.8b00040
ACS Biomater. Sci. Eng. 2018, 4, 1463−1470

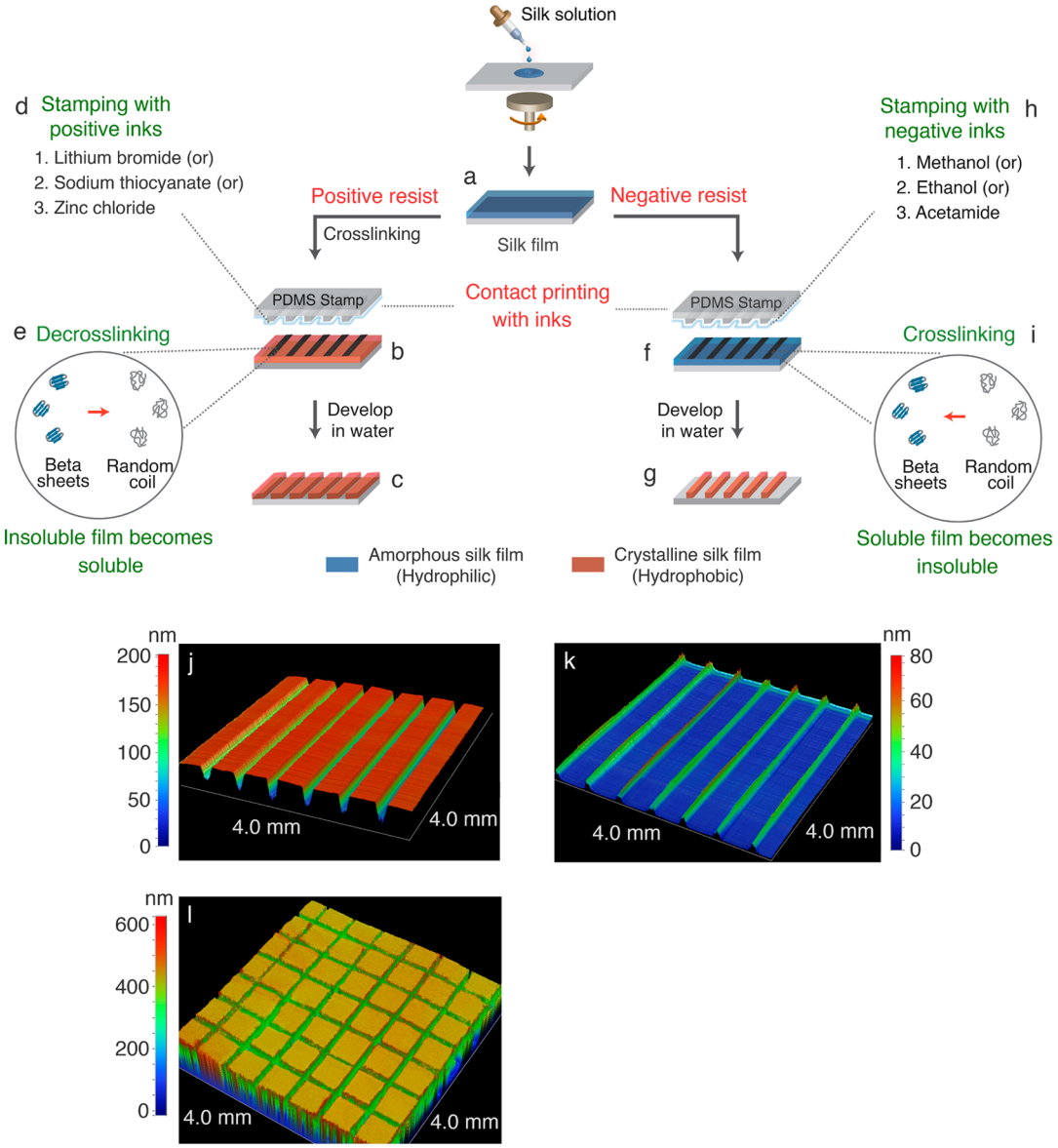

Figure 1. Schematic illustration and experimental demonstration of silk microcontact printing. (a) Spin coating of silk solution on substrate. (b) The spin-coated substrates were crosslinked using methanol and contact-printed using a PDMS (poly(dimethylsiloxane)) elastomeric stamp with the positive inks. (c) The substrate was developed with water to obtain the final pattern. During development, the water removed the amorphous silk from the substrates and generated positive patterns. (d) List of the identified positive inks. (e) In the contact-printed area, the positive inks de-crosslink the silk and convert β-sheets to random coils. (f) Contact printing of the silk film using the PDMS stamp with the negative inks. (g) The substrate was developed with water to generate the negative pattern. During development, the water removed the amorphous silk from the substrate and generated negative pattern. (h) List of identified negative inks. (i) In the contact-printed area, the negative inks crosslink silk and convert random coils into β-sheets. (j) White light interferometry images of silk structures generated by positive microcontact printing. Scale bar represents z-profile. Positive pattern was generated by stamping lithium bromide ink on crosslinked silk. (k) White light interferometry images of silk structures generated by negative microcontact printing. Scale bar represents z-profile. Negative pattern was generated by stamping acetamide ink on amorphous silk. (l) White light interferometry images of silk structures generated by positive microcontact printing. The pattern was generated iteratively using two times positive microcontact printing.

2. RESULTS AND DISCUSSION

2.1. Process Flow. The silk fibroin and ink interactions permit both positive and negative lithography by using a single stamp (Table S1). Figure 1 shows a schematic representation of the process of silk-based microcontact printing. For positive lithography, the silk fibroin solution, which was extracted from *Bombyx mori*, was spin-coated on a substrate (Figure 1a), and the substrate was crosslinked with methanol to form β-sheets. Then, the stamp was inked using an ink pad and immediately contact-printed onto the prepared substrate (Figure 1b). The positive inks de-crosslinked the silk by converting the β-sheets into random coils (Figures 1d and 1e). Consequently, the stamped area was water-soluble and removed by water (serving as the developer). The contact-printed area generated holes in the silk resist (positive pattern) (Figures 1c and 1j). For negative lithography, the silk film was deposited on the surface; then, the stamp was directly inked using the pad, and the stamp prints the features onto the silk film (Figure 1f). Because negative inks crosslink the silk (Figures 1h and 1i), the stamped area is water insoluble, and the remaining parts are removed by

DOI: 10.1021/acsbiomaterials.8b00040
ACS Biomater. Sci. Eng. 2018, 4, 1463−1470

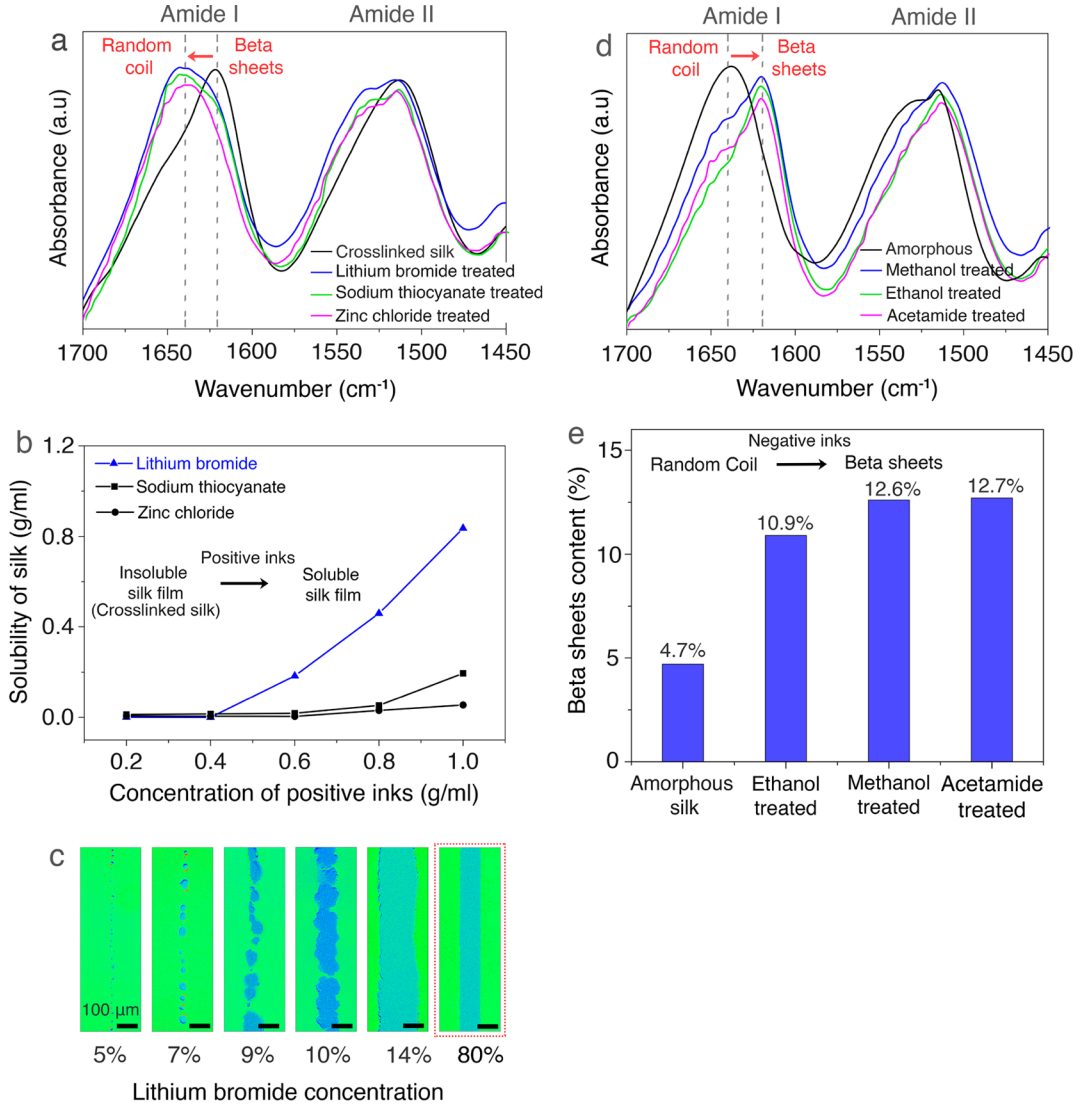

Figure 2. Mechanism of pattern formation and optimization of inks for microcontact printing. (a) Identification of positive inks using FTIR spectroscopy. Positive inks convert β-sheets to random coils. (b) Identification of the best positive inks through the solubility of the crosslinked silk. Solubility was used as the measure of de-crosslinking. (c) White light inteferometry images of optimization of the lithium bromide concentration for positive lithography. Micrographs represented with false-color for the identification of z-profile. (d) Identification of negative inks using FTIR spectroscopy. Negative inks convert random coils to β-sheets. (e) Identification of the best negative inks through FTIR deconvolution of the amide-I band. Acetamide-treated silk had the highest β-sheet content.

the water (Figure 1g). At the end of the negative lithographic process, walls were observed to have formed in the contacted areas, whereas the opposite is observed for positive lithography (Figure 1k). While in the above process silk can be used for both negative and positive microcontact printing by using a single stamp, another stamp is required to generate the inverse patterns in conventional microcontact printing. Moreover, further optimization of inks viscosity,[41] resist, and concentration of the inks can improve the resolution around nanometers.[19,42] In addition, the printing can also be iteratively done on the same silk film to generate more complex 2D patterns (Figure 1).

2.2. Materials and Optimization. For positive lithography, the inks used must de-crosslink the silk fibroin (Table S2). Whereas crosslinked silk consists mostly of β-sheets, de-crosslinked silk contains random coils. Consequently, the positive inks need to convert the β-sheets to random coils (Figure 2a). Among the various options (Table S2), lithium bromide, zinc chloride, and sodium thiocyanate rupture the inter- and intramolecular hydrogen bonds in the fibroin structure and facilitate the molecular transition from β-sheets (1620 cm^{-1}) to random coil (1638 cm^{-1}), which make them suitable inks for positive lithography (Figures S1 and S2). To analyze the effectiveness of these inks, we used solubility as a measure because the positive inks should de-crosslink and dissolve the silk (Figure 2b). The crosslinked silk becomes more soluble when the concentration of all the positive inks is increased from 0.2 to 1 g/mL for all the positive inks. At higher concentrations, lithium bromide is at least 4 times better than sodium thiocyanate and 16 times better than the zinc chloride. Therefore, we chose lithium bromide as a suitable ink for positive lithography. The concentration of the lithium bromide had a direct effect on the quality of the microcontact printed patterns (Figure 2c, Figure S3). At lower concentrations, discontinuous patterns were observed, whereas at 14 wt %, continuous patterns began to form but with poor resolution,

DOI: 10.1021/acsbiomaterials.8b00040
ACS Biomater. Sci. Eng. 2018, 4, 1463−1470

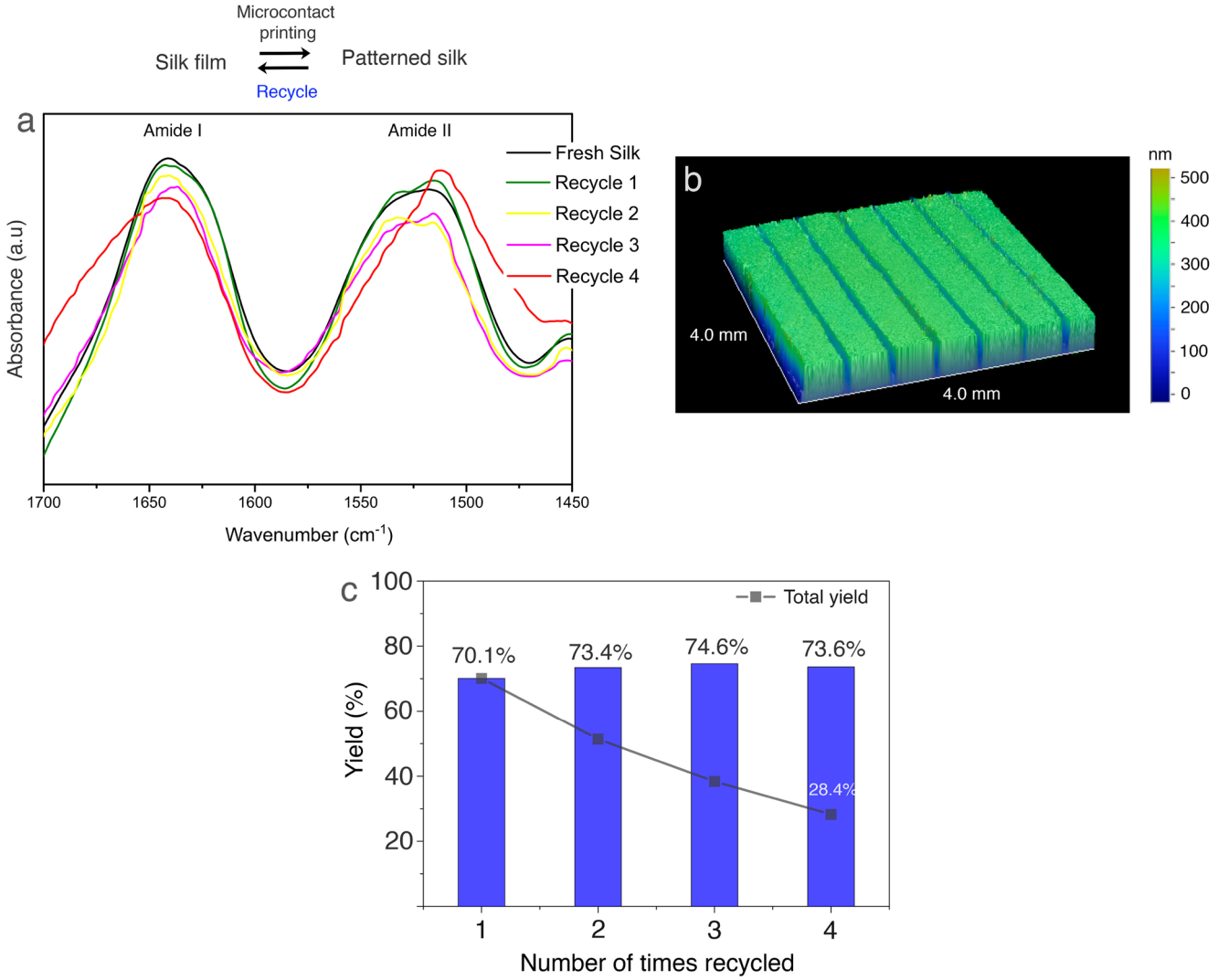

Figure 3. The silk film was recyclable after pattern generation. (a) FTIR spectrum of recycled silk. Recycled spectra of silk fibroin were similar to those of fresh fibroin. (b) Silk microcontact printing using recycled silk. We observed similar quality of pattern using recycled silk. (c) Yield quantification of recycled silk. The total yield of silk (black square) after each recycling process. Detailed information on the calculation can be found in the Supporting Information.

high edge roughness (imperfect edges), and nonreproducible patterns. At higher concentrations (ca. 80 wt % and above), due to the low dispersion of the ink (Figure S4), patterns reached a high level of reproducibility with complete silk removal on the patterned area accompanied by high edge quality (Figure S5).

For negative lithography, the negative inks must crosslink the silk via the conversion from random coils to β-sheets (Table S2). The negative inks, as identified by Fourier transform infrared (FTIR) analysis, were methanol, ethanol, and acetamide (Figure 2d). To the effectiveness of the negative inks, the β-sheet content was quantified (Figures 2e and S6) by crosslinking the silk with the negative inks and then conducting FTIR analysis, which showed the increase of the peaks corresponding to the β-sheets (Tables S3 and S4). Methanol, ethanol, and acetamide were observed to trigger β-sheet formation. Because methanol and ethanol evaporate rapidly due to their low boiling points (<80 °C), using these two solvents leads to erroneous dimensions and discontinuous patterns (Figures S7 and S8). As an alternative, to decrease the evaporation of methanol during stamping, we diluted methanol in water, which has a higher boiling point, and attempted patterning using 95% methanol. To prepare 90−95% methanol, water was used as the solvent and the silk fibroin was readily soluble in water. While we did the negative lithography, the water tries to dissolve the amorphous silk and methanol tries to crosslink the silk fibroin. Hence, there is a competition in-between these two processes. As a result, the patterns generated by the 90−95% methanol had rough edges, was discontinuous, and had poor quality (Figure S9). Comparatively, acetamide shows an adequate evaporation rate for microcontact printing due to its higher boiling point of water solution. Although water has a greater influence and causes dissolution of the silk at lower concentrations, reproducible and high-quality patterns can be achieved at higher concentrations, i.e., above 40%.

We investigated the performance of resolution by varying the silk thickness while keeping the lithium bromide concentration at 80%, which is the optimized level for printing. At high thickness levels of silk film (>800 nm), we observed the irregular edges due to limited diffusion to the edges (Figure S10a). At low thickness levels of silk film (<20 nm), we observed undesired side walls (Figure S10b). By using the silk thickness between 30 and 220 nm, we achieved regular and

DOI: 10.1021/acsbiomaterials.8b00040
ACS Biomater. Sci. Eng. 2018, 4, 1463−1470

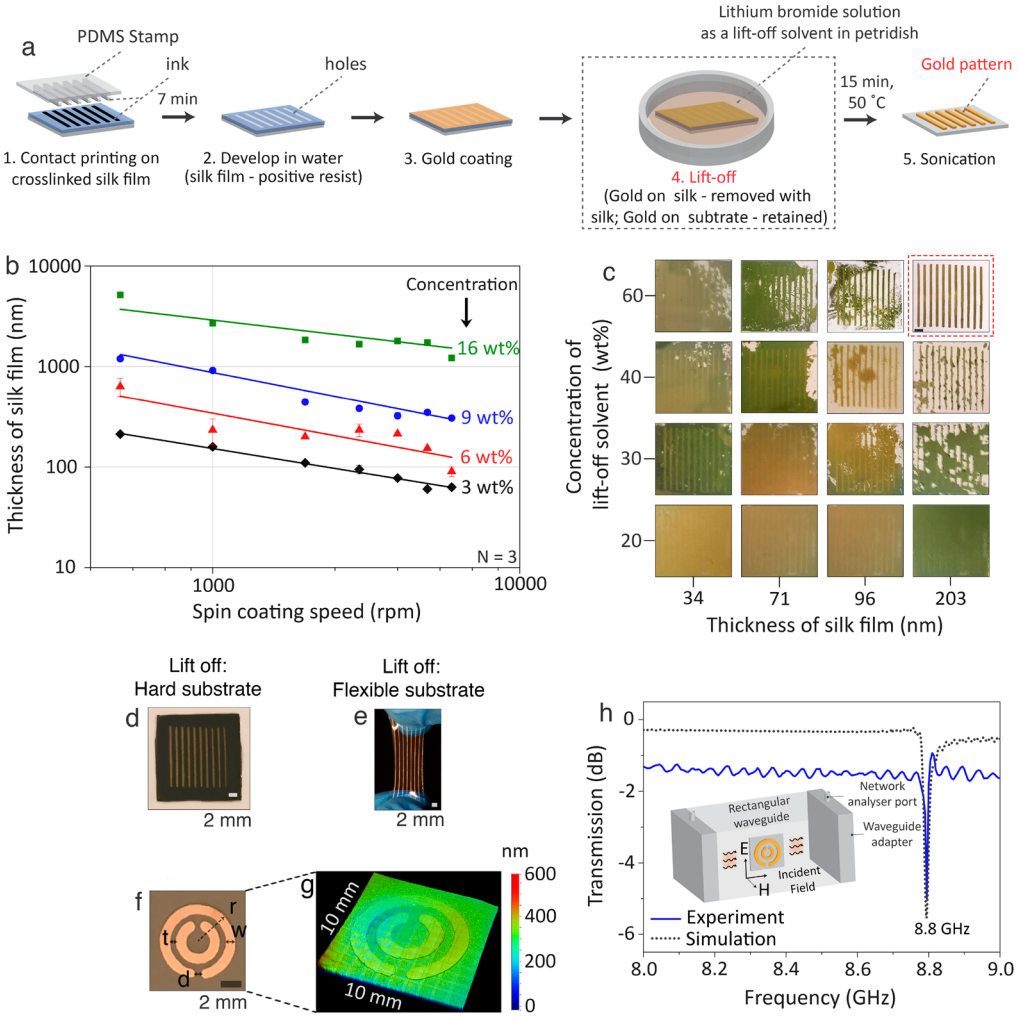

Figure 4. Metal patterning using silk microcontact printing. (a) Schematic representation of the steps involved in the patterning of a metal. (b) Silk film thickness at different spin speeds and concentrations. (c) Optimization of gold lift-off. Gold pattern was generated using the lift-off procedure. (d) Gold pattern on a hard silicon substrate and (e) gold pattern on a flexible PDMS substrate. (f) Split ring resonators (SRR) made of gold on the glass substrate. The dimensions were r = 4.03 mm, t = 0.56 mm, w = 1.08 mm, and d = 0.70 mm. (g) White light measurement of the fabricated SRR and the color bars indicate thickness. (h) The measured (blue line) and simulated (dashed black line) transmission spectra of the SRR. Inset: Schematic of the experimental setup using rectangular wave guides to measure the transmission spectrum.

well-defined edges. We anticipate that fully optimized inks with higher viscosities must result in higher resolution. To enhance the resolution, inks can be modified with additives (e.g. polymers) for desired physical properties.

2.3. Recyclability. Whereas classical resists are discarded after use, silk is recyclable after lithography (Figure 3). For recycling, the patterned silk resist needs to be initially dissolved in lithium bromide and then dialyzed to remove the side products. Because the structure and functionality of silk were not significantly changed after each recycling step (Figure 3a), the recycled silk can be reused for patterning (Figure 3b). We observed that silk is recyclable after patterning with an approximate yield of 70% (Figure 3c). Hence, after 4 cycles, 28.3% of silk remained. Furthermore, the nonrecycled parts will also safely degrade in nature due to the bio-origin of the silk fibroin protein. Therefore, silk represents an exceptional and ecofriendly resist material for microcontact printing

2.4. Metal Lift-off and Functional Metallic Structures. In electronic device fabrication, metal lift-off from the substrate is a key step in generating functional metallic structures (e.g., electrical contacts) and requires the simultaneous removal of the resist and metal top-coating from the substrate using a specific solvent (the lift-off solvent). Thus, we developed a metal lift-off procedure that is applicable to both hard and soft substrates for silk microcontact printing (Figure 4a). Initially, silk was spin-coated on glass and cross-linked with methanol. Then, the stamp, which had been inked with lithium bromide, was contact-printed on the silk resist, and then the substrate was developed with water, which dissolves the areas that interacted with lithium bromide. Gold (~60 nm) was deposited on the generated pattern, and the silk was lifted off by submersion in the lithium bromide solution for 15 min (at 50 °C). Finally, gold patterns were obtained by sonicating samples for 1 min (at 50 °C) in water. The obtained pattern was consistent with the dimensions of the prepared stamp with an error of less than 2% (Table S5). We alternatively explored a method of achieving metal lift-off without developing the substrates after contact printing (without step 2 in Figure 4a; Figure S11), but the final pattern quality was not as high as that of the water-developed substrates. We also further checked the interaction between the gold and substrate. For that, we carried out an experiment by soaking the patterned gold substrates for

DOI: 10.1021/acsbiomaterials.8b00040
ACS Biomater. Sci. Eng. 2018, 4, 1463−1470

10 min. We could not observe the gold floating by the lift off solvent. Only the silk was lifted off from the substrate, and patterns were intact (Figure S12). It is worth mentioning that adhesion of gold on the substrate can be further improved by adding an intermediate layer of titanium or chromium.

Because the thickness of the resist affects the metal lift-off process, we controlled the thickness by modifying the silk concentration and spin speed (Figure 4b). At the same concentration, the resist thickness increases when the spin speed was lowered, whereas the thickness decreased when the spin speed was increased. The concentration of the silk can also be modified to change the resulting silk resist thickness. The film thickness can be decreased by diluting silk with water, allowing the resist thickness to be varied from 62 to 5163 nm when varied silk concentrations (3−16 wt %) and spin speeds (500−5000 rpm) were used. Therefore, the tunable range covers resist thicknesses from tens of nanometers to micrometers.

Both the concentration of the lift-off solution (lithium bromide) and the silk film thickness need to be optimized to achieve a high-quality lift-off process (Figure 4c). Although at lower concentration of lithium bromide (<40 wt %), lift-off was effective; at higher concentrations (>60 wt %), the gold was etched (Figure S13). Because of the trade-off between the effectiveness of the lift-off process and protection of the metal, concentrations around 60% were established as a good interval for the lift-off procedure. Moreover, the thickness of the silk film also influences the lift-off procedure. Notably, for thicknesses above 250 nm, imperfect side edges were observed in the developed pattern, whereas thickness below 100 nm prevent the effective removal of the silk film from the top metal coating. Ultimately, we determined that a 203 nm-thick silk resist, a 60 nm-thick gold layer on silk, and 60%-concentrated lift-off solvent is an appropriate combination for the lift-off process. Moreover, the same patterning and lift-off procedure also worked on solid silicon wafers and flexible PDMS substrates (Figures 4d and 4e). By searching for a general rule of thumb for the lift-off process, we determined that in general, the lift-off of the silk requires a resist at least three times thicker than the gold coating.

We demonstrate a proof of concept of the silk lift-off process by fabricating the planar split-ring resonator (SRR) structure, which is landmark in the development of the electromagnetic metamaterials.[43−46] The magnetic resonance of the SRR serves to create an effective permeability for the medium consisting of two- or three-dimensional periodic arrays of SRRs. Hence, the fabrication of an SRR and demonstration of its magnetic resonance is the primary requirement toward the fabrication of an electromagnetic metamaterial. We designed a single SRR (Figure 4f) and 1 × 2 SRR arrays (Figures S14 and S15) made of gold on 1 mm-thick glass substrates (with the dimensions of r = 4.03 mm, t = 0.56 mm, w = 1.08 mm, and d = 0.70 mm). Figure 4g shows that the designed dimensions were transferred to the substrates and that the edges of the structures were smooth. The transmission spectrum measurements were performed using a network analyzer (Figure 4h, inset), and the SRR samples were placed within a rectangular waveguide with the magnetic field vector of the electromagnetic wave normal to the substrate plane. In this configuration, the SRR coupled to the magnetic field and exhibited a resonance frequency at 8.8 GHz (Figure 4h), which was also confirmed using the numerical simulation. A control measurement was performed with the incident signal normal to the SRR plane (Figure S16), and in this case, the resonance disappeared, indicating that the resonance had originated from magnetic coupling. In this study, the silk lift-off procedure is optimized for the fabrication of planar metallic structures with a high uniformity under a typical resolution of 100 μm. This encourages the application of the method to other electromagnetic devices which involve planar metallic features at comparable scales. In particular, printed (microstrip) antenna structures and phased array antenna structures can benefit from the proposed fabrication method.

2.5. Applicability in Resource Limited Settings. Many of the state-of-the-art techniques, such as E-beam lithography (EBL) and EUV lithography, require expensive tools and are used to obtain high-resolution patterns. Instead, silk microcontact printing is a simple, transportable, and cheap method to produce patterns for the applications, which do not require that much high-level resolution. Moreover, many of the necessary materials (e.g., silk, water, etc.) that are required in silk microcontact printing are globally accessible. For example, in Africa, silk production is a well-established industry, and hence the necessary silk can be generated locally. For pattern generation, the work on silk-based EBL[19,47] uses the water and silk that do not require special waste management. The microcontact printing uses common laboratory solvents in addition to water and silk. In comparison with EBL, it is simple, transportable, and low-cost method without the requirement for any expensive equipment. The procedure is inexpensive (4 cents/print, Table S6), and the lack of a requirement for sophisticated skills increases the potential of this technique.

Although the present method explores initial steps in development of lithography for resource-limited settings, few issues need to be addressed to make the method truly effective for the resource limited settings. First, the spin coater used in the process may not be readily available at resource limited settings, but it can be realized using a potter's wheel-like device construction or modified egg beater.[48] The master stamp, salts, common chemicals, and other items involved in the printing can be easily transported due to no requirement for cold-chain transportation, like the previous methods.[2,5] For the resource limited settings, negative ink alcohol can be obtained through distillation of ethanol from alcoholic beverages. One remaining point is the hygroscopic nature of positive inks, which can be solved by packing the inks as one time usable small containers. Moreover, the method and necessary components may be alternatively offered as a complete kit (Figure S17).

3. CONCLUSION

In conclusion, silk microcontact printing that uses silk, water, and common laboratory solvents was demonstrated. It provides a simple, ecofriendly, recyclable, configurable, and biocompatible lithographic technique. Silk-ink interactions and lift-off procedure were optimized to generate the functional structures. The present method offers unusual lithographic capabilities that can be utilized for applications ranging from electronics to biological interfaces. Because the present method requires ordinary laboratory materials and basic skills, this method may find widespread use in resource-limited settings. Moreover, new procedures can be further developed for producing integrated circuits, microelectromechanical systems (MEMS), optics, and surface engineering.

DOI: 10.1021/acsbiomaterials.8b00040
ACS Biomater. Sci. Eng. 2018, 4, 1463−1470

■ ASSOCIATED CONTENT

Supporting Information

The Supporting Information is available free of charge on the ACS Publications website at DOI: 10.1021/acsbiomaterials.8b00040.

Details on the experimental procedures and supporting data (PDF)

■ AUTHOR INFORMATION

Corresponding Author

*E-mail: snizamoglu@ku.edu.tr.

ORCID

Rustamzhon Melikov: 0000-0003-2214-7604
Sadra Sadeghi: 0000-0002-8569-1626
Kaan Guven: 0000-0002-1097-5106
Sedat Nizamoglu: 0000-0003-0394-5790

Notes

The authors declare no competing financial interest.

■ ACKNOWLEDGMENTS

This project received funding from the European Research Council (ERC) under the European Union's Horizon 2020 research and innovation programme (Grant no 639846). We thank Prof. Ismail Lazgolu and Muzaffer Butun for helping to make the master macro stamps; Dr. Daniel Aaron Press and Dr. Sven Holmstrom of Koc University, Turkey, for the valuable discussions about making the micro master stamp; and Ms.Itir Bakis Dogru and Prof. Emel Yilgor for the contact angle measurements.

■ REFERENCES

(1) Pollock, N. R.; Rolland, J. P.; Kumar, S.; Beattie, P. D.; Jain, S.; Noubary, F.; Wong, V. L.; Pohlmann, R. A.; Ryan, U. S.; Whitesides, G. M. A paper-based multiplexed transaminase test for low-cost, point-of-care liver function testing. *Sci. Transl. Med.* **2012**, *4* (152), 152ra129−152ra129.

(2) Nemiroski, A.; Christodouleas, D. C.; Hennek, J. W.; Kumar, A. A.; Maxwell, E. J.; Fernández-Abedul, M. T.; Whitesides, G. M. Universal mobile electrochemical detector designed for use in resource-limited applications. *Proc. Natl. Acad. Sci. U. S. A.* **2014**, *111* (33), 11984−11989.

(3) Sia, S. K.; Linder, V.; Parviz, B. A.; Siegel, A.; Whitesides, G. M. An Integrated Approach to a Portable and Low-Cost Immunoassay for Resource-Poor Settings. *Angew. Chem., Int. Ed.* **2004**, *43* (4), 498−502.

(4) Drain, P. K.; Hyle, E. P.; Noubary, F.; Freedberg, K. A.; Wilson, D.; Bishai, W. R.; Rodriguez, W.; Bassett, I. V. Diagnostic point-of-care tests in resource-limited settings. *Lancet Infect. Dis.* **2014**, *14* (3), 239−249.

(5) Mudanyali, O.; Dimitrov, S.; Sikora, U.; Padmanabhan, S.; Navruz, I.; Ozcan, A. Integrated rapid-diagnostic-test reader platform on a cellphone. *Lab Chip* **2012**, *12* (15), 2678−2686.

(6) Mudanyali, O.; Tseng, D.; Oh, C.; Isikman, S. O.; Sencan, I.; Bishara, W.; Oztoprak, C.; Seo, S.; Khademhosseini, B.; Ozcan, A. Compact, light-weight and cost-effective microscope based on lensless incoherent holography for telemedicine applications. *Lab Chip* **2010**, *10* (11), 1417−1428.

(7) Zhu, H.; Yaglidere, O.; Su, T.-W.; Tseng, D.; Ozcan, A. Cost-effective and compact wide-field fluorescent imaging on a cell-phone. *Lab Chip* **2011**, *11* (2), 315−322.

(8) He, Q.; Ma, C.; Hu, X.; Chen, H. Method for fabrication of paper-based microfluidic devices by alkylsilane self-assembling and UV/O3-patterning. *Anal. Chem.* **2013**, *85* (3), 1327−1331.

(9) Martinez, A. W.; Phillips, S. T.; Butte, M. J.; Whitesides, G. M. Patterned paper as a platform for inexpensive, low-volume, portable bioassays. *Angew. Chem., Int. Ed.* **2007**, *46* (8), 1318−1320.

(10) Martinez, A. W.; Phillips, S. T.; Whitesides, G. M. Three-dimensional microfluidic devices fabricated in layered paper and tape. *Proc. Natl. Acad. Sci. U. S. A.* **2008**, *105* (50), 19606−19611.

(11) Kumar, A. A.; Chunda-Liyoka, C.; Hennek, J. W.; Mantina, H.; Lee, S. R.; Patton, M. R.; Sambo, P.; Sinyangwe, S.; Kankasa, C.; Chintu, C. Evaluation of a density-based rapid diagnostic test for sickle cell disease in a clinical setting in Zambia. *PLoS One* **2014**, *9* (12), e114540.

(12) Kumar, A. A.; Patton, M. R.; Hennek, J. W.; Lee, S. Y. R.; D'Alesio-Spina, G.; Yang, X.; Kanter, J.; Shevkoplyas, S. S.; Brugnara, C.; Whitesides, G. M. Density-based separation in multiphase systems provides a simple method to identify sickle cell disease. *Proc. Natl. Acad. Sci. U. S. A.* **2014**, *111* (41), 14864−14869.

(13) Xia, Y.; Whitesides, G. M. Soft lithography. *Annu. Rev. Mater. Sci.* **1998**, *28* (1), 153−184.

(14) Perl, A.; Reinhoudt, D. N.; Huskens, J. Microcontact printing: limitations and achievements. *Adv. Mater.* **2009**, *21* (22), 2257−2268.

(15) Gassensmith, J. J.; Erne, P. M.; Paxton, W. F.; Frasconi, M.; Donakowski, M. D.; Stoddart, J. F. Patterned assembly of quantum dots onto surfaces modified with click microcontact printing. *Adv. Mater.* **2013**, *25* (2), 223−226.

(16) Frederico, G. *An Economic History of the Silk Industry*; Cambridge University Press: Cambridge, 1997.

(17) Omenetto, F. G.; Kaplan, D. L. New opportunities for an ancient material. *Science* **2010**, *329* (5991), 528−531.

(18) Sun, Y.-L.; Li, Q.; Sun, S.-M.; Huang, J.-C.; Zheng, B.-Y.; Chen, Q.-D.; Shao, Z.-Z.; Sun, H.-B. Aqueous multiphoton lithography with multifunctional silk-centred bio-resists. *Nat. Commun.* **2015**, *6*, 1 DOI: 10.1038/ncomms9612.

(19) Kim, S.; Marelli, B.; Brenckle, M. A.; Mitropoulos, A. N.; Gil, E.-S.; Tsioris, K.; Tao, H.; Kaplan, D. L.; Omenetto, F. G. All-water-based electron-beam lithography using silk as a resist. *Nat. Nanotechnol.* **2014**, *9* (4), 306−310.

(20) Mondia, J. P.; Amsden, J. J.; Lin, D.; Negro, L. D.; Kaplan, D. L.; Omenetto, F. G. Rapid nanoimprinting of doped silk films for enhanced fluorescent emission. *Adv. Mater.* **2010**, *22* (41), 4596−4599.

(21) Lee, W.; Zhang, S.; Liu, M.; Tao, T. H. Near-field thermal nanolithography using silk proteins. *CLEO: Applications and Technology* **2016**, *JW2A*, 106.

(22) Bae, W. K.; Kwak, J.; Park, J. W.; Char, K.; Lee, C.; Lee, S. Highly Efficient Green-Light-Emitting Diodes Based on CdSe@ ZnS Quantum Dots with a Chemical-Composition Gradient. *Adv. Mater.* **2009**, *21* (17), 1690−1694.

(23) Bucciarelli, A.; Pal, R. K.; Maniglio, D.; Quaranta, A.; Mulloni, V.; Motta, A.; Yadavalli, V. K. Fabrication of Nanoscale Patternable Films of Silk Fibroin Using Benign Solvents. *Macromol. Mater. Eng.* **2017**, *302*, 1700110.

(24) Park, J.; Choi, Y.; Lee, M.; Jeon, H.; Kim, S. Novel and simple route to fabricate fully biocompatible plasmonic mushroom arrays adhered on silk biopolymer. *Nanoscale* **2015**, *7* (2), 426−431.

(25) Morikawa, J.; Ryu, M.; Maximova, K.; Balčytis, A.; Seniutinas, G.; Fan, L.; Mizeikis, V.; Li, J.; Wang, X.; Zamengo, M. Silk fibroin as a water-soluble bio-resist and its thermal properties. *RSC Adv.* **2016**, *6* (14), 11863−11869.

(26) Pal, R. K.; Kurland, N. E.; Wang, C.; Kundu, S. C.; Yadavalli, V. K. Biopatterning of silk proteins for soft micro-optics. *ACS Appl. Mater. Interfaces* **2015**, *7* (16), 8809−8816.

(27) Dickerson, M. B.; Dennis, P. B.; Tondiglia, V. P.; Nadeau, L. J.; Singh, K. M.; Drummy, L. F.; Partlow, B. P.; Brown, D. P.; Omenetto, F. G.; Kaplan, D. L. 3D Printing of Regenerated Silk Fibroin and Antibody-Containing Microstructures via Multiphoton Lithography. *ACS Biomater. Sci. Eng.* **2017**, *3* (9), 2064−2075.

(28) Tao, H.; Marelli, B.; Yang, M.; An, B.; Onses, M. S.; Rogers, J. A.; Kaplan, D. L.; Omenetto, F. G. Inkjet printing of regenerated silk

DOI: 10.1021/acsbiomaterials.8b00040
ACS Biomater. Sci. Eng. 2018, 4, 1463−1470

fibroin: From printable forms to printable functions. *Adv. Mater.* **2015**, *27* (29), 4273−4279.
(29) Suntivich, R.; Drachuk, I.; Calabrese, R.; Kaplan, D. L.; Tsukruk, V. V. Inkjet printing of silk nest arrays for cell hosting. *Biomacromolecules* **2014**, *15* (4), 1428−1435.
(30) Young, S. L.; Gupta, M.; Hanske, C.; Fery, A.; Scheibel, T.; Tsukruk, V. V. Utilizing conformational changes for patterning thin films of recombinant spider silk proteins. *Biomacromolecules* **2012**, *13* (10), 3189−3199.
(31) Gupta, M. K.; Singamaneni, S.; McConney, M.; Drummy, L. F.; Naik, R. R.; Tsukruk, V. V. A facile fabrication strategy for patterning protein chain conformation in silk materials. *Adv. Mater.* **2010**, *22* (1), 115−119.
(32) Schacht, K.; Jüngst, T.; Schweinlin, M.; Ewald, A.; Groll, J.; Scheibel, T. Biofabrication of Cell-Loaded 3D Spider Silk Constructs. *Angew. Chem., Int. Ed.* **2015**, *54* (9), 2816−2820.
(33) DeSimone, E.; Schacht, K.; Jungst, T.; Groll, J.; Scheibel, T. Biofabrication of 3D constructs: Fabrication technologies and spider silk proteins as bioinks. *Pure Appl. Chem.* **2015**, *87* (8), 737−749.
(34) Perry, H.; Gopinath, A.; Kaplan, D. L.; Dal Negro, L.; Omenetto, F. G. Nano-and micropatterning of optically transparent, mechanically robust, biocompatible silk fibroin films. *Adv. Mater.* **2008**, *20* (16), 3070−3072.
(35) Brenckle, M. A.; Tao, H.; Kim, S.; Paquette, M.; Kaplan, D. L.; Omenetto, F. G. Protein-Protein Nanoimprinting of Silk Fibroin Films. *Adv. Mater.* **2013**, *25* (17), 2409−2414.
(36) Khang, D. Y.; Yoon, H.; Lee, H. H. Room-Temperature Imprint Lithography. *Adv. Mater.* **2001**, *13* (10), 749−752.
(37) Park, J.; Lee, S.-G.; Marelli, B.; Lee, M.; Kim, T.; Oh, H.-K.; Jeon, H.; Omenetto, F. G.; Kim, S. Eco-friendly photolithography using water-developable pure silk fibroin. *RSC Adv.* **2016**, *6* (45), 39330−39334.
(38) Kurland, N. E.; Dey, T.; Kundu, S. C.; Yadavalli, V. K. Precise patterning of silk microstructures using photolithography. *Adv. Mater.* **2013**, *25* (43), 6207−6212.
(39) Kurland, N. E.; Dey, T.; Wang, C.; Kundu, S. C.; Yadavalli, V. K. Silk protein lithography as a route to fabricate sericin micro-architectures. *Adv. Mater.* **2014**, *26* (26), 4431−4437.
(40) Xia, Y.; Rogers, J. A.; Paul, K. E.; Whitesides, G. M. Unconventional methods for fabricating and patterning nanostructures. *Chem. Rev.* **1999**, *99* (7), 1823−1848.
(41) Lessing, J.; Glavan, A. C.; Walker, S. B.; Keplinger, C.; Lewis, J. A.; Whitesides, G. M. Inkjet Printing of Conductive Inks with High Lateral Resolution on Omniphobic "RF Paper" for Paper-Based Electronics and MEMS. *Adv. Mater.* **2014**, *26* (27), 4677−4682.
(42) Schmid, H.; Michel, B. Siloxane polymers for high-resolution, high-accuracy soft lithography. *Macromolecules* **2000**, *33* (8), 3042−3049.
(43) Shelby, R. A.; Smith, D. R.; Schultz, S. Experimental verification of a negative index of refraction. *Science* **2001**, *292* (5514), 77−79.
(44) Guven, K.; Caliskan, M. D.; Ozbay, E. Experimental observation of left-handed transmission in a bilayer metamaterial under normal-to-plane propagation. *Opt. Express* **2006**, *14* (19), 8685−8693.
(45) Pendry, J. B.; Holden, A. J.; Robbins, D.; Stewart, W. Magnetism from conductors and enhanced nonlinear phenomena. *IEEE Trans. Microwave Theory Tech.* **1999**, *47* (11), 2075−2084.
(46) Aydin, K.; Bulu, I.; Guven, K.; Kafesaki, M.; Soukoulis, C. M.; Ozbay, E. Investigation of magnetic resonances for different split-ring resonator parameters and designs. *New J. Phys.* **2005**, *7* (1), 168.
(47) Qin, N.; Zhang, S.; Jiang, J.; Corder, S. G.; Qian, Z.; Zhou, Z.; Lee, W.; Liu, K.; Wang, X.; Li, X. Nanoscale probing of electron-regulated structural transitions in silk proteins by near-field IR imaging and nano-spectroscopy. *Nat. Commun.* **2016**, *7*, 13079.
(48) Wong, A. P.; Gupta, M.; Shevkoplyas, S. S.; Whitesides, G. M. Egg beater as centrifuge: isolating human blood plasma from whole blood in resource-poor settings. *Lab Chip* **2008**, *8* (12), 2032−2037.

DOI: 10.1021/acsbiomaterials.8b00040
ACS Biomater. Sci. Eng. 2018, 4, 1463−1470